Journal of Computational Physics **170,** 320–337 (2001)
doi:10.1006/jcph.2001.6739, available online at http://www.idealibrary.com on IDEAL®

Surface-Tension-Driven Convection in a Fluid Overlying a Porous Layer

B. Straughan

Department of Mathematical Sciences, University of Durham, Durham DH1 3LE, United Kingdom
E-mail: Brian.Straughan@durham.ac.uk

Received August 8, 2000; revised January 12, 2001

An accurate numerical analysis for the onset of thermal convection in a two-layer system is presented. The system comprises a saturated porous layer over which lies a layer of the same fluid. The layered system is heated from below, the upper (fluid) surface is free to the atmosphere, and convection driven by surface tension is allowed for. The eigenvalues and eigenfunctions for the instability problem are derived by utilizing a D^2 Chebyshev tau method (J. J. Dongarra, B. Straughan, and D. W. Walker, 1996, *Appl. Numer. Math.* **22**, 399–435). This allows us to obtain highly accurate eigenvalues and eigenfunctions in a very efficient manner. The onset of convection is seen to have a bimodal nature in which convection may be dominated by the porous medium or by the fluid, depending on the depths of the relative layers and the strength of the tension in the fluid surface. The effect of surface tension is investigated in detail and it is found that for the parameter $\hat{d}$ (=depth of fluid layer/depth of porous layer) very small, the surface tension has a strong effect on convection dominated by the porous medium, whereas for $\hat{d}$ larger the surface tension effect is observed only with the fluid mode.

Key Words: Chebyshev tau method; superposed porous–fluid convection; surface tension; multilayer convection; Marangoni effect.

1. INTRODUCTION

In 1988, Chen and Chen [4] produced a classical paper in which they studied thermal convection in a two-layer system composed of a porous layer saturated with fluid over which was a layer of the same (clear) fluid. The layer was heated from below and Chen and Chen [4] considered the bottom of the porous layer, as well as the upper surface of the fluid, to be fixed. They showed that the linear instability curves for the onset of convective motion, i.e., the Rayleigh number against wavenumber curves, may be bimodal in that the curves

0021-9991/01 $35.00

possess two local minima. A crucial parameter in their analysis is the number

$$\hat{d} = \frac{d}{d_m} = \frac{\text{depth of fluid layer}}{\text{depth of porous layer}}. \tag{1.1}$$

They interpreted their findings by showing that for $\hat{d}$ small (≤ 0.13) the instability was initiated in the porous medium, whereas for $\hat{d}$ larger than this the mechanism changed and instability was controlled by the fluid layer. The work of Chen and Chen [4] employed the fundamental model for convection in a porous–fluid-layer system developed originally by Nield [11]. Thus, in turn, it employed the experimentally suggested condition at the interface between the porous and the fluid media proposed by Beavers and Joseph [1],

$$\frac{\partial u^\beta}{\partial z} = \frac{\alpha}{\sqrt{K}}\left(u^\beta - u_m^\beta\right), \quad \beta = 1, 2. \tag{1.2}$$

In this equation u^β are the x and y components of the fluid velocity u^i, u_m^β are the equivalent components of the fluid velocity in the porous medium u_m^i, α is a constant depending on the porous medium, and K is the permeability. This equation holds along the horizontal interface between the porous medium and the fluid, z being in the vertical direction.

Since the problem of convection in a porous–fluid system is one with many industrial and geophysical applications, it has received much attention in the literature (cf. the review of Nield [15] and the book by Nield and Bejan [16]). Nield [11–14] studied in much detail systems of two or more layers especially with regard to which porous-medium model is most appropriate for convection. Blest *et al.* [2, 3] considered a very interesting application to the manufacture of composite materials used in the aircraft and automobile industries. McKay [10] considered a problem similar to that of Chen and Chen [4] but with chemical reactions allowed in the layers. Many other references may be found in these papers.

The purposes of this article are twofold: one is to derive a D^2 Chebyshev tau method (cf. Dongarra *et al.* [6] and Straughan and Walker [19]) to yield eigenvalues and eigenfunctions accurately for the two-layer problem, and the other is to investigate in detail the physically important problem where the upper (fluid) surface is free and the surface tension, being temperature dependent, may influence convective motion. The latter aspect is timely because Nield [14] (see also the references therein) specifically addressed the question of modelling convection in a porous medium when the upper surface is free. We pay particular attention to the case of $\hat{d}$ small, approximately equal to 0.005, and thus obtain numerical information on Nield's model.

The implementation of a D^2 Chebyshev tau method is, we believe, highly useful in porous–fluid convection problems. Chen and Chen [4] employed a shooting method. The D^2 method given here has several advantages. Apart from numerical accuracy, we are able to calculate as many eigenvalues as we need, which is useful when the eigenvalues of interest are changing in parameter space. We can also calculate the eigenfunctions very easily.

In this work we also employ the Beavers–Joseph condition (1.2). Payne and Straughan [17] have shown that the solution to thermal flow problems depends continuously on the parameter α when Darcy's law is adopted in the porous medium and Stokes's flow holds in the fluid layer. Indeed, the Beavers–Joseph condition has proved successful in other slow-flow situations, such as flow past a porous sphere (see Qin and Kaloni [18]). However, the analysis of [17] casts serious doubt on whether (1.2) would be realistic for larger fluid velocities for which Navier–Stokes flow is valid. Since we restrict attention here to the

onset of surface-tension-driven convection in the porous–fluid system, our analysis is one of linearised instability and so we effectively consider Stokes's flow. Hence, use of (1.2) is justified.

We shall employ the notation of Chen and Chen [4] except for the surface tension part, which is new. Hence, we consider a porous medium occupying the layer $z \in (-d_m, 0)$ with the fluid in the layer $z \in (0, d)$. Naturally, the interface is at $z = 0$. The equations in the fluid are the Navier–Stokes equations

$$\begin{aligned} \frac{\partial u_i}{\partial t} + u_j \frac{\partial u_i}{\partial x_j} &= -\frac{1}{\rho_0}\frac{\partial p}{\partial x_i} + \nu \Delta u_i + \bar{\alpha} g T k_i, \\ \frac{\partial u_i}{\partial x_i} &= 0, \\ \frac{\partial T}{\partial t} + u_i \frac{\partial T}{\partial x_i} &= \frac{k_f}{(\rho_0 c_p)_f} \Delta T, \end{aligned} \tag{1.3}$$

holding for time $t > 0$, in the spatial domain $\{(x, y) \in \mathbb{R}^2, z \in (0, d)\}$. In these equations u_i, p, and T are velocity, pressure, and temperature and ρ_0, ν, $\bar{\alpha}$, g, k_f, and c_p are density, kinematic viscosity, thermal expansion coefficient, gravity, thermal conductivity, and specific heat at constant pressure. Standard indicial notation is employed throughout, subscript f or m denotes fluid or porous medium, respectively, $k = (0, 0, 1)$, and Δ is the Laplace operator.

In the porous medium the equations are

$$\begin{aligned} \frac{1}{\phi}\frac{\partial u_i^m}{\partial t} &= -\frac{1}{\rho_0}\frac{\partial p^m}{\partial x_i} - \frac{\nu}{k} u_i^m + \bar{\alpha} g T_m k_i, \\ \frac{\partial u_i^m}{\partial x_i} &= 0, \\ (\rho_0 c_p)^* \frac{\partial T_m}{\partial t} + (\rho_0 c_p)_f u_i^m \frac{\partial T_m}{\partial x_i} &= k^* \Delta T_m, \end{aligned} \tag{1.4}$$

with $t > 0$, and $\mathbf{x} \in \{(x, y) \in \mathbb{R}^2, z \in (-d_m, 0)\}$. The quantities u_i^m, p_m, and T_m are respectively velocity, pressure, and temperature in the porous medium, ϕ is the porosity, and

$$X^* = \phi X_f + (1 - \phi) X_m,$$

where in (1.4) X is replaced by k or $\rho_0 c_p$.

The steady-state solution in whose stability we are interested is one for which there is no fluid motion in either layer and the temperatures at the upper and lower boundaries are held at fixed constant temperatures T_U and T_L, respectively, with $T_L > T_U$.

The basic steady-state solution to Eqs. (1.3) and (1.4) is found as in Chen and Chen [4]. It is this solution which we examine for linearised instability. In fact, the basic solution $(\bar{u}_i, \bar{T}, \bar{p})$, $(\bar{u}_i^m, \bar{T}^m, \bar{p}^m)$, is the same as in Chen and Chen [4], so

$$\begin{aligned} \bar{u}_i = 0, \qquad \bar{u}_i^m = 0, \\ \bar{T} = T_0 - (T_0 - T_U)\frac{z}{d}, \quad 0 \le z \le d, \\ \bar{T}_m = T_0 - (T_L - T_0)\frac{z}{d_m}, \quad -d_m \le z \le 0. \end{aligned} \tag{1.5}$$

Here T_0 is the temperature at the interface, which is found by requiring continuity of temperature and heat flux as (cf. [4])

$$T_0 = \frac{k^* d T_L + k_f d_m T_U}{k^* d + k_f d_m}. \tag{1.6}$$

We note that $T_L > T_0$ and $T_0 > T_U$. The steady pressures $\bar{p}$ and $\bar{p}^m$ are found from (1.3) and (1.4). Since these are not required explicitly in the ensuing instability analysis, we do not give them.

There are two fundamental differences from the Chen and Chen [4] situation. One of these is the surface-tension condition at the stress-free fluid surface, which is discussed in the next section. The other concerns the temperature field at the fluid surface $z = d$. At this surface a radiation-type boundary condition of the form

$$\delta_1 \frac{d\bar{T}}{dz} + \delta_2 \bar{T} = c, \quad \text{at } z = d, \tag{1.7}$$

in the steady state is assumed. The coefficients δ_1 and δ_2 depend on exactly what conditions hold in the atmosphere. For example, in bright sunshine δ_1 is large since heating is mainly by radiation, whereas under cloudy or foggy conditions δ_2 will be dominant. The term c is prescribed. It is convenient to rewrite δ_1 and δ_2 in terms of a constant L as

$$\delta_1 = \frac{1}{1+L}, \qquad \delta_2 = \frac{L}{1+L}, \tag{1.8}$$

and then if $\bar{T}(d) = T_U$, from (1.7) we find

$$c(1+L) = L T_U + \left(\frac{T_U - T_0}{d} \right),$$

which yields

$$T_U = \frac{cd(1+L) + T_0}{1 + Ld}. \tag{1.9}$$

Thus, for given c we always know T_U, and this is consistent with the Chen and Chen [4] steady solution, provided T_U is interpreted as in (1.9). Again, the continuity of heat flux condition

$$k_f \frac{d\bar{T}}{dz} = k^* \frac{d\bar{T}_m}{dz} \quad \text{at } z = 0$$

yields the steady solution (1.5), (1.6) as in Chen and Chen [4].

In the next section we derive equations for a perturbation (u_i, θ, π) to $(\bar{u}_i, \bar{T}, \bar{p})$ and (u_i^m, θ_m, π_m) to $(\bar{u}_i^m, \bar{T}_m, \bar{p}_m)$. In terms of the perturbation θ, the boundary condition (1.7) leads to a condition on the temperature field at the fluid surface of the form

$$\frac{\partial \theta}{\partial z} + L\theta = 0, \quad \text{on } z = d. \tag{1.10}$$

The boundary conditions on the velocity in the steady state are $w_m = 0$ at $z = -d_m$, where $w_m = u_3^m$, $\mathbf{u} \cdot \mathbf{n}$ is continuous at $z = 0$, and $\mathbf{n} = (0, 0, 1)$. The stress-free condition on u_i at $z = d$ is considered together with the other boundary conditions in the next section.

2. PERTURBATION EQUATIONS FOR THE LINEAR INSTABILITY PROBLEM

We now put $u_i = \bar{u}_i + u_i$, $T = \bar{T} + \theta$, $p = \bar{p} + \pi$, $u_i^m = \bar{u}_i^m + u_i^m$, $T_m = \bar{T}_m + \theta_m$, and $p_m = \bar{p}_m + \pi_m$ in (1.3) and (1.4) and derive *linearised* equations for the perturbation quantities $(u_i, \theta, \pi, u_i^m, \theta_m, \pi_m)$. Although these equations are formally the same as those in [4], we do include a derivation. The reason is that in [4] the time derivative terms are ignored in deriving the boundary conditions and a *priori* we cannot do this. For surface-tension-driven convection in a pure fluid (cf. [5, 8]) under suitable conditions, one may find that convective motion commences by oscillatory convection. Thus, we derive the boundary conditions at the outset retaining time-derivative terms.

The linearised perturbation equations from (1.3) and (1.4) are, after introducion of a time dependence, of the form

$$u_i = u_i(\mathbf{x})e^{\sigma t}, \quad \theta = \theta(\mathbf{x})e^{\sigma t}, \quad u_i^m = u_i^m(\mathbf{x})e^{\sigma_m t}, \quad \theta_m = \theta_m(\mathbf{x})e^{\sigma_m t},$$

$$\begin{aligned} \rho_o \sigma u_i &= -\frac{\partial \pi}{\partial x_i} + \mu \Delta u_i + \rho_0 \bar{\alpha} g k_i \theta, \\ \frac{\partial u_i}{\partial x_i} &= 0, \\ \sigma \theta &= \left(\frac{T_0 - T_U}{d} \right) w + \frac{k_f}{(\rho_0 c_p)_f} \Delta \theta, \end{aligned} \tag{2.1}$$

$$\begin{aligned} \frac{\rho_0}{\phi} \sigma_m u_i^m &= -\frac{\partial \pi^m}{\partial x_i} - \frac{\mu}{k} u_i^m + \rho_0 \bar{\alpha} g k_i \theta_m, \\ \frac{\partial u_i^m}{\partial x_i} &= 0, \\ \sigma_m \theta_m &= \left(\frac{T_L - T_0}{d_m} \right) \frac{(\rho_0 c_p)_f}{(\rho_0 c_p)^*} w_m + \frac{k^*}{(\rho_0 c_p)^*} \Delta \theta_m, \end{aligned} \tag{2.2}$$

where $w = u_3$, $w_m = u_3^m$, and $\mu = \nu \rho_0$ is the dynamic viscosity.

In fact, we employ the nondimensionalization of Chen and Chen [4] and after using the normal modes to represent the x and y dependence, in terms of fluid and porous wavenumbers a and a_m, we derive exactly the same equations from (2.1) and (2.2) as those of [4, Eqs. (26), (27), (29), and (30)]. Thus, with

$$w = W(z) f(x, y), \quad \theta = \Theta(z) f(x, y), \quad w_m = W_m(z) f(x, y), \quad \theta_m = \Theta_m(z) f(x, y),$$

f being the horizontal planform, the eigenvalue equations for the growth rates σ and σ_m are

$$\begin{aligned} (D^2 - a^2)^2 W - a^2 Ra \Theta &= \frac{\sigma}{Pr} (D^2 - a^2) W, \\ (D^2 - a^2)\Theta - W &= \sigma \Theta, \end{aligned} \tag{2.3}$$

$$\begin{aligned} \left(D^2 - a_m^2\right) W_m + a_m^2 Ra_m \Theta_m &= -\sigma_m \frac{\delta^2}{\phi Pr_m} \left(D^2 - a_m^2\right) W_m, \\ \left(D^2 - a_m^2\right) \Theta_m - W_m &= \sigma_m G_m \Theta_m. \end{aligned} \tag{2.4}$$

In (2.3), $D = d/dz$, with (2.3) holding in $z \in (0,1)$, whereas (2.4) hold in $z_m \in (-1,0)$ and $D = d/dz_m$. The quantities Ra and Ra_m are the Rayleigh number and porous Rayleigh number given by

$$Ra = \frac{g\bar{\alpha}\rho_0(T_U - T_0)d^3(\rho_0 c_p)_f}{\mu k_f}, \tag{2.5}$$

$$Ra_m = Ra\frac{(\delta\epsilon_T)^2}{\hat{d}^4}. \tag{2.6}$$

Note that Ra and Ra_m are *negative*. The quantities Pr and Pr_m the Prandtl and porous Prandtl numbers, δ is the Darcy number given by $\delta = \sqrt{k}/d_m$, and

$$G_m = \frac{(\rho_0 c_p)^*}{(\rho_0 c_p)\,f}, \quad \epsilon_T = \frac{\lambda_f}{\lambda_m},$$

with the fluid and porous medium thermal diffusivities being defined by $\lambda_f = k_f/(\rho_0 c_p)_f$ and $\lambda_m = k^*/(\rho_0 c_p)^*$.

Equations (2.3) and (2.4) form a tenth-order system to be solved for the eigenvalue σ (or σ_m, which is related) with Ra, Ra_m, and the other parameters fixed. In fact, σ and σ_m are related as

$$\sigma_m = \frac{\hat{d}^2}{\epsilon_T}\sigma.$$

Minimisation is performed in a or a_m. For this we need 10 boundary conditions. On $z = -1$, the bottom of the porous layer, we have

$$W_m = \Theta_m = 0, \quad z = -1. \tag{2.7}$$

On the upper (fluid) surface $z = 1$, we have

$$W = 0, \quad D\Theta + L\Theta = 0, \quad z = 1, \tag{2.8}$$

and at the interface continuity of normal velocity, temperature, and the heat flux, yields

$$W = \hat{d}W_m, \quad \hat{d}\Theta = \epsilon_T^2\Theta_m, \quad D\Theta = \epsilon_T D_p\Theta_m, \quad z = 0, \tag{2.9}$$

where we observe that the interface between the fluid and porous media is $z = 0$ and we have accentuated the derivative d/dz_m by employing D_p for this.

Two further interface conditions and one further condition on $z = 1$ are needed.

To derive the condition on $z = 1$ we suppose the surface tension, σ, to have the form

$$\sigma = \sigma_0[1 - \gamma(T - T_0)], \tag{2.10}$$

where σ_0 and γ are constants. If t^i and t_{ij} denote the stress vector and stress tensor, then at $z = 1$,

$$t^i = t_{ij}n_j = \sigma b^\alpha_\alpha n^i + x^i_{;\alpha}a^{\alpha\beta}\sigma_{;\beta}, \tag{2.11}$$

where b^α_α is the mean curvature of the surface, $x^i_{;\alpha}$ are tangential vectors, $a^{\alpha\beta}$ is the first fundamental form of the surface, and $;\alpha$ denotes covariant differentiation with respect to the surface coordinates. Since in the fluid

$$t_{ij} = -p\delta_{ij} + 2\mu d_{ij}, \qquad d_{ij} = \frac{1}{2}(u_{i,j} + u_{j,i}),$$

condition (2.11) on $z = 0$ becomes

$$-pn^i + \mu\left(\frac{\partial u_i}{\partial z} + \frac{\partial w}{\partial x_i}\right) = \sigma b^\alpha_\alpha n^i + x^i_{;\alpha} a^{\alpha\beta}\sigma_{;\beta}.$$

The horizontal components, $i = 1, 2$, of this yield for the perturbation quantities

$$\mu\frac{\partial u}{\partial z} = -\gamma\sigma_0\frac{\partial\theta}{\partial x}, \qquad \mu\frac{\partial v}{\partial z} = -\gamma\sigma_0\frac{\partial\theta}{\partial y}.$$

These are added and nondimensionalized, and the condition $u_{i,i} = 0$ is employed to deduce

$$D^2W = Ma\Delta^*\theta, \quad \text{on } z = 1. \tag{2.12}$$

Here, $\Delta^* = \partial^2/\partial x^2 + \partial^2/\partial y^2$ and Ma is the Marangoni number,

$$Ma = \frac{\gamma\sigma_0(T_U - T_0)d}{\lambda_f\mu}. \tag{2.13}$$

Note that since we are heating from below, in this work $Ma < 0$.

To derive the interface boundary conditions we start with the Beavers–Joseph condition

$$\frac{\partial u_\beta}{\partial z} = \frac{\alpha}{\sqrt{k}}(u_\beta - u^m_\beta), \quad \beta = 1, 2, \text{ on } z = 0.$$

The equation for $\beta = 1$ is differentiated with respect to x, that for $\beta = 2$ is differentiated with respect to y, and the results are added. Using the fact that $u_{i,i} = 0$, one derives the nondimensional form

$$D^2W - \frac{\alpha\hat{d}}{\delta}DW + \frac{\alpha\hat{d}^3}{\delta}D_pW_m = 0. \tag{2.14}$$

Continuity of normal stress at the interface requires

$$n_i t^i_m = n_i t^i_f,$$

where t^i_m and t^i_f are the stress vectors in the porous and fluid media. Here,

$$n_i t^i_f = -\pi^m\delta_{i3}n_i$$

and

$$n_i t^i_f = -(\pi^f\delta_{i3} - 2\mu d_{i3})n_i.$$

Thus, we find

$$\pi^m = \pi - 2\mu\frac{\partial w}{\partial z}, \quad \text{on } z = 0. \tag{2.15}$$

We take $\partial/\partial x_\alpha$ of this, $\alpha = 1, 2$, to find

$$\frac{\partial \pi^m}{\partial x_\alpha} = \frac{\partial \pi}{\partial x_\alpha} - 2\mu \frac{\partial^2 w}{\partial x_\alpha \partial z}, \quad \text{on } z = 0. \tag{2.16}$$

Then, we substitute from the differential equations $(2.1)_1$ and $(2.2)_1$ for $\pi_{,\alpha}$ and $\pi^m_{,\alpha}$. Using $u_{\alpha,\alpha} = -w_{,z}$ we derive, in nondimensional form, the final interface condition

$$\frac{\hat{d}^4}{\phi Pr_m}\sigma_m D_p W^m + \frac{\hat{d}^4}{\delta^2} D_p W^m = \frac{1}{Pr}\sigma DW - D^3 W - 3\Delta^* DW, \quad \text{on } z = 0. \tag{2.17}$$

It is important to note that σ and σ_m do appear in the boundary condition (2.17). Chen and Chen [4] searched directly for instabilities when $\sigma, \sigma_m \in \mathbb{R}$ and therefore they discarded the σ terms in (2.17).

Thus, the complete eigenvalue system to be solved comprises (2.3), (2.4), (2.7), (2.8), (2.9), (2.12), (2.14), and (2.17). The numerical method for this is described in the next section.

3. NUMERICAL METHOD

We now briefly describe the numerical method employed to solve the eigenvalue problem of Section 2. We implement a D^2 variant of the Chebyshev tau method (cf. Dongarra *et al.* [6]). The implementation of this is important since it is a highly accurate method which yields eigenvalues and eigenfunctions easily, and we believe its use in multilayer porous-fluid problems has much potential.

We first transform (2.3) to the Chebyshev domain $(-1, 1)$ by putting $\hat{z} = 2z - 1$ and then transform (2.4) to the same domain with the transformation $\hat{z}_m = -2z_m - 1$. This means that the fluid surface $z = 1$ becomes $\hat{z} = 1$ and the porous surface $z_m = -1$ becomes $\hat{z}_m = 1$ while the interface $z = 0 = z_m$ becomes $\hat{z} = -1 = \hat{z}_m$. Equations (2.3) are written as three systems of second-order equations, namely

$$\begin{aligned} (D^2 - a^2)W - A &= 0, \\ (D^2 - a^2)A - a^2 Ra\Theta &= \frac{\sigma}{Pr}A, \\ (D^2 - a^2)\Theta - W &= \sigma\Theta, \end{aligned} \tag{3.1}$$

while (2.4) are already in second-order form. On $z = 1$ we have the boundary conditions (2.8) and (2.12), whereas on $z_m = -1$, (2.7) hold. On the interface $z = 0$, the five boundary conditions are (2.9), (2.14), and (2.17). Of course, Eqs. (3.1) and (2.4) and the boundary conditions must also be transformed to their appropriate domains.

The five variables W, A, Θ, W_m, and Θ_m are then regarded as independent and are expanded as Chebyshev series

$$\begin{gathered} W = \sum_{n=0}^{N+2} W_n T_n(z), \qquad A = \sum_{n=0}^{N+2} A_n T_n(z), \qquad \Theta = \sum_{n=0}^{N+2} \Theta_n T_n(z), \\ W_m = \sum_{n=0}^{N+2} W_n^m T_n(z), \qquad \Theta_m = \sum_{n=0}^{N+2} \Theta_n^m T_n(z). \end{gathered} \tag{3.2}$$

The operator D^2 is written in matrix form (cf. [6]) and the $m(N+1)$ and $m(N+2)$ rows of the resulting matrix, $m = 1, \ldots, 5$, are replaced with the boundary conditions, recalling $T_n(\pm 1) = (\pm 1)^n$ and $T_n'(\pm 1) = (\pm 1)^{n-1} n^2$. This gives rise to a generalised $5(N+3) \times 5(N+3)$ matrix eigenvalue problem of the form

$$A\mathbf{x} = \sigma B\mathbf{x}. \tag{3.3}$$

This generalised matrix eigenvalue problem is solved with the aid of the QZ algorithm.

In many hydrodynamic stability eigenvalue studies there has been a serious problem with so-called spurious eigenvalues (cf. Dongarra *et al.* [6], Gardner *et al.* [7], McFadden *et al.* [9], Straughan and Walker [19], and Zebib [22]. These are not true eigenvalues of the system but are artefacts of the approximation process. One of the major reasons given for the appearance of spurious eigenvalues is the occurrence of zero rows in B because of the boundary conditions (cf. [6, 7, 9, 19, 22]). We should point out that with the system (3.3) which arises in this study, we *can* remove offending boundary condition terms from the B matrix, albeit at technical expense. However, since in our numerical calculations we do not witness the production of spurious eigenvalues, we have not done so and have simply employed the boundary conditions as the $m(N+1)$th and $m(N+2)$th rows of A and (where appropriate) B. We do not have a rigorous explanation for the nonappearance of spurious eigenvalues, but we believe that they are not witnessed because of the mathematical nature of the problem under investigation. While the eigenvalues require care for their accurate computation, the eigenfunctions are not nearly linearly dependent as they are in parallel flow problems as studied in e.g., [6, 7, 22]. It would appear that the nonnormality of the operators associated with parallel flow problems has a significant bearing on the presence of spurious eigenvalues.

4. NUMERICAL RESULTS

One interesting fact we observed in our computations was that the critical eigenvalue σ was real, even with surface tension present, although we are restricting attention to the case of heating from below. This is important from the viewpoint of the results of Chen and Chen [4] in that it justifies their procedure of taking σ real from the outset.

In our numerical results we have taken $Pr = 6$, a figure consistent with water being the working fluid. We choose $\delta = 0.002, \epsilon_T = 0.7, G_m = 10, \phi = 0.3,$ and $\alpha = 0.1$, which are figures consistent with many porous materials as described by Chen and Chen [4] and Beavers and Joseph [1]. The radiation value of $L = 10$ is selected; again this is typical of real situations (cf. [5, 8]). This paper concentrates on varying the depth ratio $\hat{d}$ and the surface-tension effect through the Marangoni number Ma.

Figures 1a and 1b show, for fixed $Ma = -100$, the effect of $\hat{d}$ variation. When $\hat{d} = 0.05$ and 0.07, the critical value of Ra_m is for $a_m = 2.0$ and 2.0, respectively, as shown in Table I. This means that convection is dominated by the porous medium as might be expected since the fluid layer is relatively thin. When $\hat{d} = 0.09, 0.11,$ and 0.13 (the graphs are shown in greater detail in Fig. 1b), the critical Ra_m values are, respectively, for $a_m = 23.5, 19.5, 17.0$, and therefore the convective motion is initiated by the fluid layer. Thus, there is a critical $\hat{d}$ somewhere between 0.07 and 0.09 for which the instability switches from being dominated by the porous layer with small wavenumber (wider convection cells)

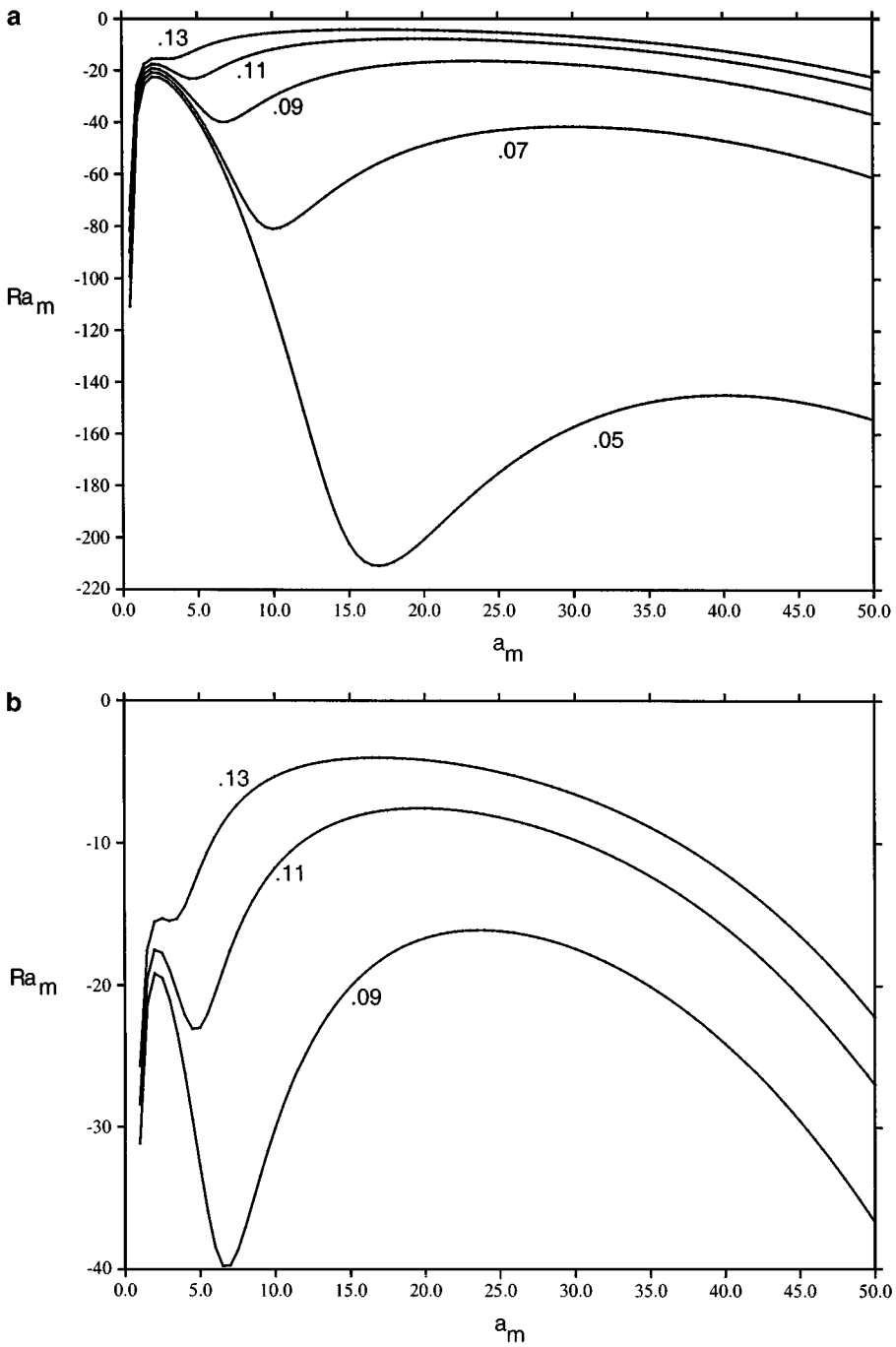

FIG. 1. Critical porous Rayleigh number against porous wavenumber. (a) $Pr = 6$, $G_m = 10$, $\epsilon_T = 0.7$, $\phi = 0.3$, $Ma = -100$, $\alpha = 0.1$, $\delta = 0.002$, $L = 10$, $\hat{d}$ values on graphs; (b) $Pr = 6$, $G_m = 10$, $\epsilon_T = 0.7$, $\phi = 0.3$, $Ma = -100$, $\alpha = 0.1$, $\delta = 0.002$, $L = 10$, $\hat{d}$ values on graphs.

TABLE I
Maximum Values of Ra_m with the Corresponding Values of a_m

$\hat{d}$	Ra_m	a_m	Ra_m	a_m
0.05	−22.55	2.0	−144.81	40
0.07	−20.77	2.0	−41.49	30
0.09	−19.17	2.0	−16.12	23.5
0.11	−17.53	2.0	−7.54	19.5
0.13	No	Minimum	−4.00	17.0

Note. $Pr = 6$, $G_m = 10$, $\epsilon_T = 0.7$, $\phi = 0.3$, $Ma = -100$, $\alpha = 0.1$, $\delta = 0.002$, $L = 10$.

to being dominated by the fluid layer with much larger wavenumbers (thin convection cells). This bimodal neutral curve behaviour was known before (cf. [4]), but we confirm it even when surface tension is acting on the upper surface. The Rayleigh and wavenumbers are essentially discontinuous in $\hat{d}$.

Figures 2–5 display the effect of changing surface tension while keeping $\hat{d}$ fixed. When $\hat{d} = 0.03$ and 0.05 we see that convection is always dominated by the porous medium, at least for $Ma \geq -400$. Precise values for the maximum of these curves are given in Tables II and III.

Figure 4, for $\hat{d} = 0.07$, is interesting: we observe that the porous layer dominates the convection for $Ma = 0, -100, -200,$ and -300. However, when $Ma = -400$ instability commences through the fluid layer. This can be understood more easily from Table IV. Thus, the effect of increasing surface tension eventually allows the fluid layer to dominate convective motion.

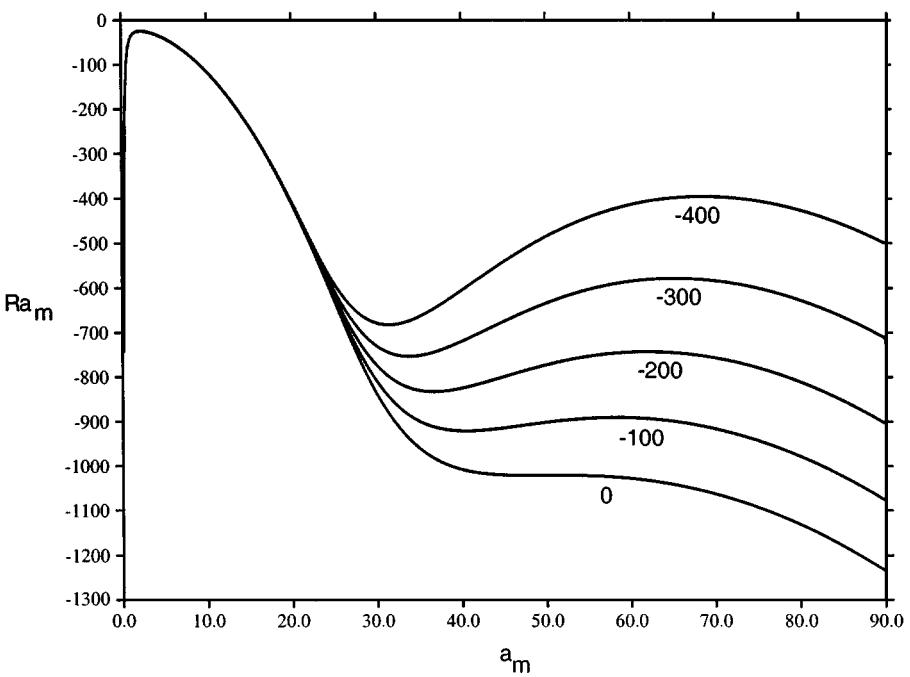

FIG. 2. Critical porous Rayleigh number against porous wavenumber. $Pr = 6$, $G_m = 10$, $\epsilon_T = 0.7$, $\phi = 0.3$, $\hat{d} = 0.03$, $\alpha = 0.1$, $\delta = 0.002$, $L = 10$, Ma values on graphs.

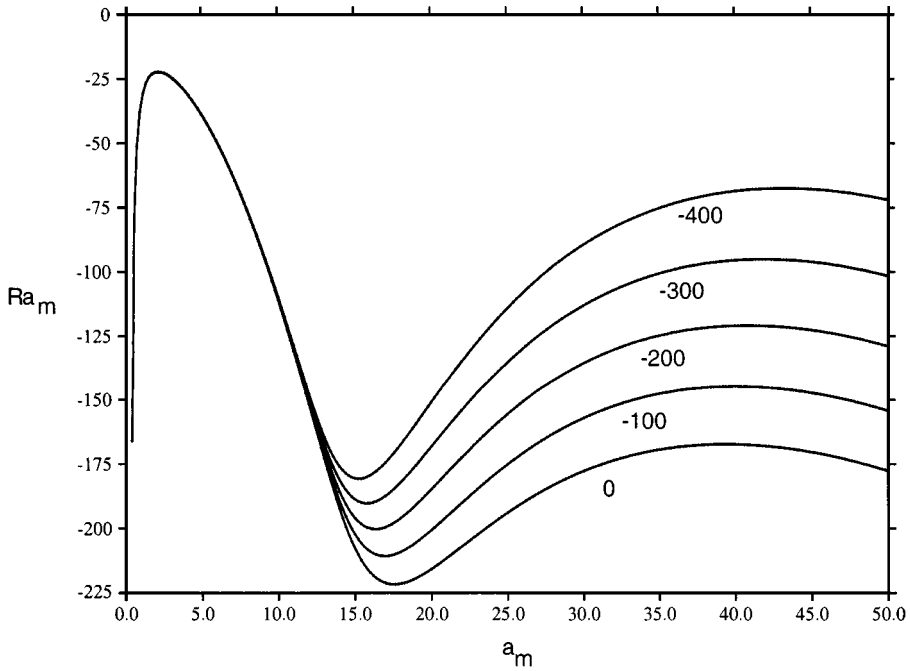

FIG. 3. Critical porous Rayleigh number against porous wavenumber. $Pr = 6$, $G_m = 10$, $\epsilon_T = 0.7$, $\phi = 0.3$, $\hat{d} = 0.05$, $\alpha = 0.1$, $\delta = 0.002$, $L = 10$, *Ma* values on graphs.

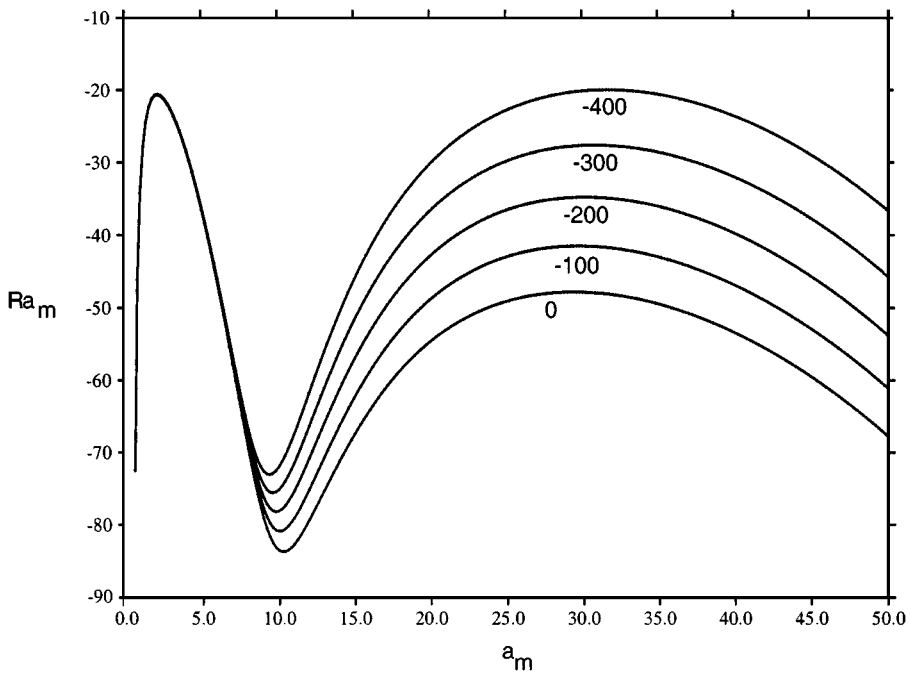

FIG. 4. Critical porous Rayleigh number against porous wavenumber. $Pr = 6$, $G_m = 10$, $\epsilon_T = 0.7$, $\phi = 0.3$, $\hat{d} = 0.07$, $\alpha = 0.1$, $\delta = 0.002$, $L = 10$, *Ma* values on graphs.

TABLE II

Maximum Values of Ra_m with the Corresponding Values of a_m

Ma	Ra_m	a_m	Ra_m	a_m
0	−24.66	2.4	−1020.87	51.4
−100	−24.52	2.4	−890.47	58.2
−200	−24.39	2.4	−742.70	62.0
−300	−24.25	2.4	−578.26	65.2
−400	−24.11	2.4	−395.44	68.6

Note. $Pr = 6,\ G_m = 10,\ \epsilon_T = 0.7,\ \phi = 0.3,\ \hat{d} = 0.03,\ \alpha = 0.1,\ \delta = 0.002,\ L = 10.$

TABLE III

Maximum Values of Ra_m with the Corresponding Values of a_m

Ma	Ra_m	a_m	Ra_m	a_m
0	−22.396	2.2	−167.28	39.4
−100	−22.342	2.2	−144.807	40.0
−200	−22.287	2.2	−120.841	40.8
−300	−22.233	2.2	−95.163	41.8
−400	−22.178	2.2	−67.477	43.2

Note. $Pr = 6,\ G_m = 10,\ \epsilon_T = 0.7,\ \phi = 0.3,\ \hat{d} = 0.05,\ \alpha = 0.1,\ \delta = 0.002,\ L = 10.$

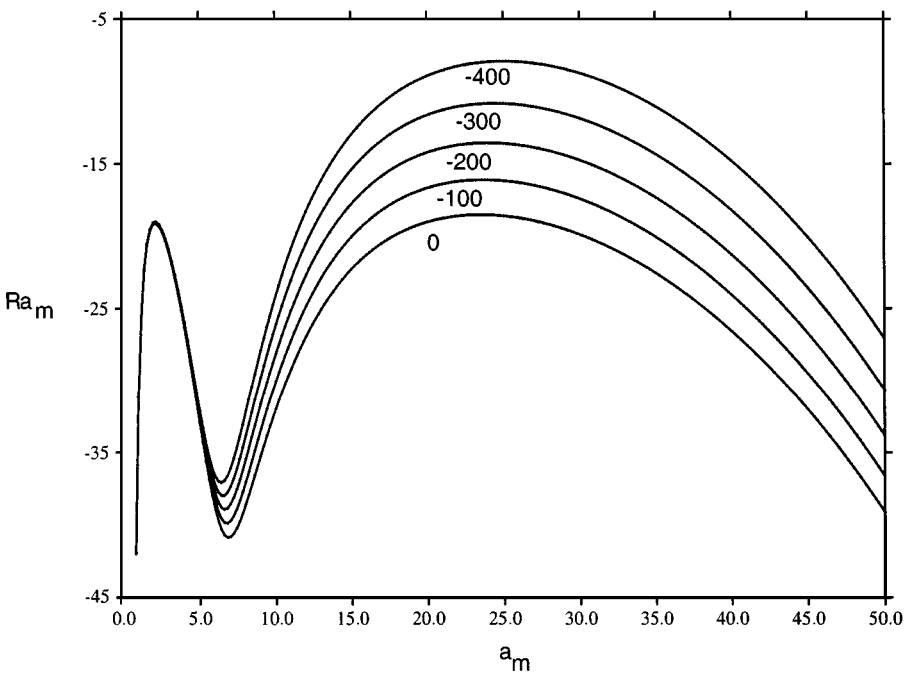

FIG. 5. Critical porous Rayleigh number against porous wavenumber. $Pr = 6,\ G_m = 10,\ \epsilon_T = 0.7,\ \phi = 0.3,\ \hat{d} = 0.09,\ \alpha = 0.1,\ \delta = 0.002,\ L = 10,\ Ma$ values on graphs.

TABLE IV
Maximum Values of Ra_m with the Corresponding Values of a_m

Ma	Ra_m	a_m	Ra_m	a_m
0	−20.690	2.2	−47.814	29.4
−100	−20.656	2.2	−41.491	29.8
−200	−20.622	2.2	−34.780	30.2
−300	−20.588	2.2	−27.628	30.8
−400	−20.553	2.2	−19.962	31.6

Note. $Pr = 6,\ G_m = 10,\ \epsilon_T = 0.7,\ \phi = 0.3,\ \hat{d} = 0.07,\ \alpha = 0.1,\ \delta = 0.002,\ L = 10.$

When $\hat{d} = 0.09$, then all five cases, $Ma = 0, \ldots, -400$, are such that the fluid layer dominates the convection. Numerical values for the maximum of the curves are given in Table V.

Figures 6a and 6b display the velocity, W, W_m, eigenfunction and demonstrate how the situation for Fig. 4 with $\hat{d} = 0.07$ changes when Ma switches from -300 to -400. In Fig. 6a, we see that for $Ma = -400$ the motion is almost entirely in the fluid layer whereas for $Ma = -300$ the porous layer has a strong effect. In Fig. 7a, the temperature variation in the fluid layer is dominant when $Ma = -400$ whereas for $Ma = -300$ (see Fig. 7b) the temperature variation in the porous layer is important.

The effect of $\hat{d}$ being very small is considered in Table VI. For $Ma \geq -400$, the convection is dominated by the porous medium. However, we are able to ascertain the surface-tension effect quite strongly. When $\hat{d} = 0.01$ we see a 10.45% variation in Ra_m as Ma varies from 0 to -400, when $\hat{d} = 0.005$ this variation is 17.11%, and when $\hat{d} = 0.004$ the variation is 18.55%. Clearly, as the fluid layer becomes very thin, the effect of surface tension will play an important role, as we expect physically. Certainly, for a porous layer of depth 2 cm (typical in laboratory experiments) when $\hat{d} = 0.005$, this means the porous medium is covered by a fluid layer of depth 0.1 mm. This is effectively a thin film, and we do expect surface tension to have an effect.

Throughout our calculations we have been able to obtain highly accurate results with very few polynomials. Mostly we employed 30 polynomials and so the matrix sizes in (3.3) are 150×150. With modern computers this allows us to obtain neutral curves such as those in Figs. 1–5 in a reasonable time. For $\hat{d} = 0.005$ and 0.004 we required 50 polynomials for reasonable accuracy and we found it difficult to proceed for $\hat{d}$ smaller than this.

TABLE V
Maximum Values of Ra_m with the Corresponding Values of a_m

Ma	Ra_m	a_m	Ra_m	a_m
0	−19.13	2.2	−18.53	23.4
−100	−19.10	2.2	−16.11	23.6
−200	−19.07	2.2	−13.56	24.0
−300	−19.04	2.2	−10.84	24.4
−400	−19.01	2.2	−7.93	25.0

Note. $Pr = 6, G_m = 10, \epsilon_T = 0.7, \phi = 0.3, \hat{d} = 0.09, \alpha = 0.1, \delta = 0.002,$ $L = 10.$

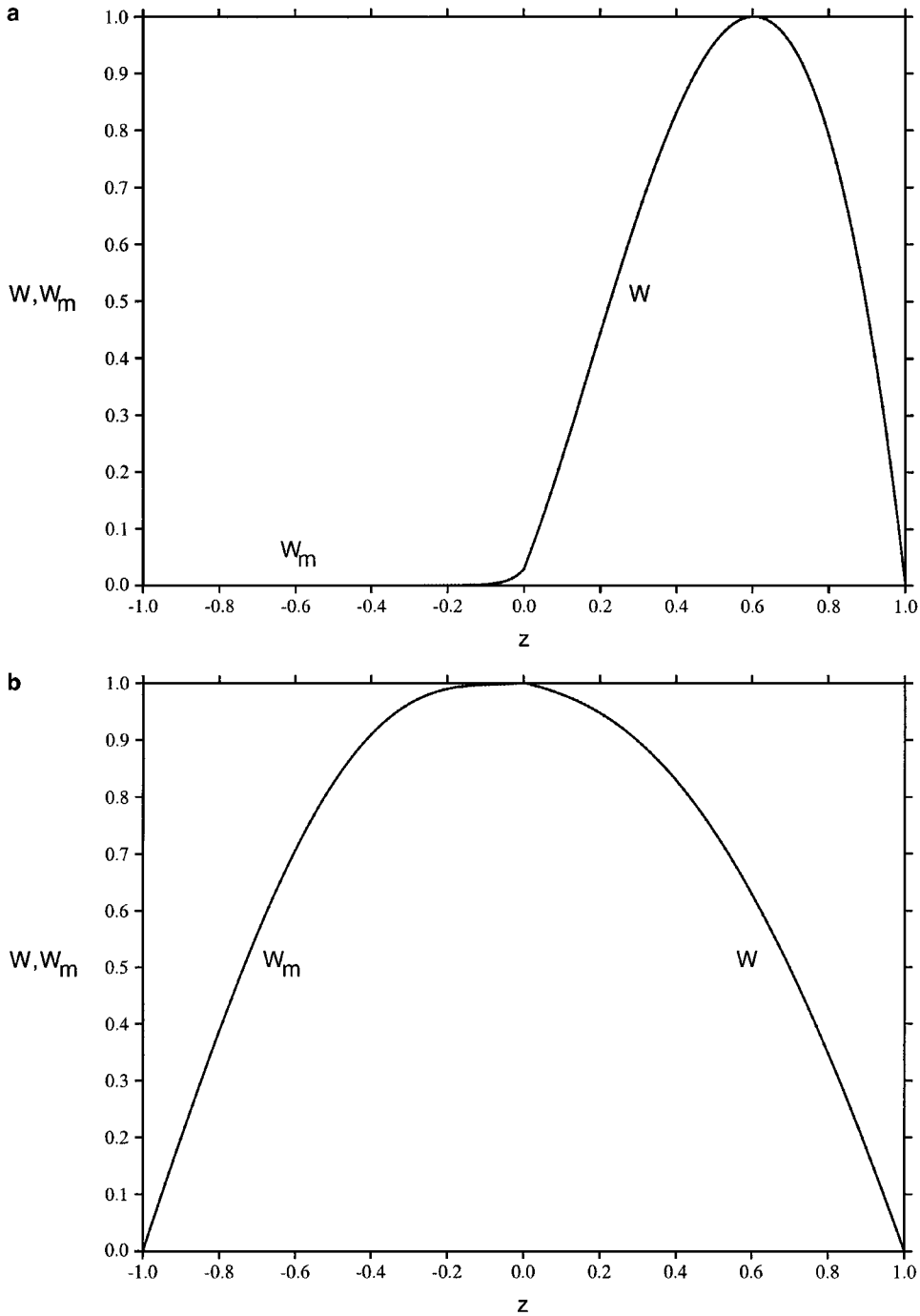

FIG. 6. Dimensional eigenfunctions W and W_m. (a) $Pr = 6, G_m = 10, \epsilon_T = 0.7, \phi = 0.3, \hat{d} = 0.07, \alpha = 0.1, \delta = 0.002, L = 10, Ma = -400$; (b) $Pr = 6, G_m = 10, \epsilon_T = 0.7, \phi = 0.3, \hat{d} = 0.09, \alpha = 0.1, \delta = 0.002, L = 10, Ma = -300$.

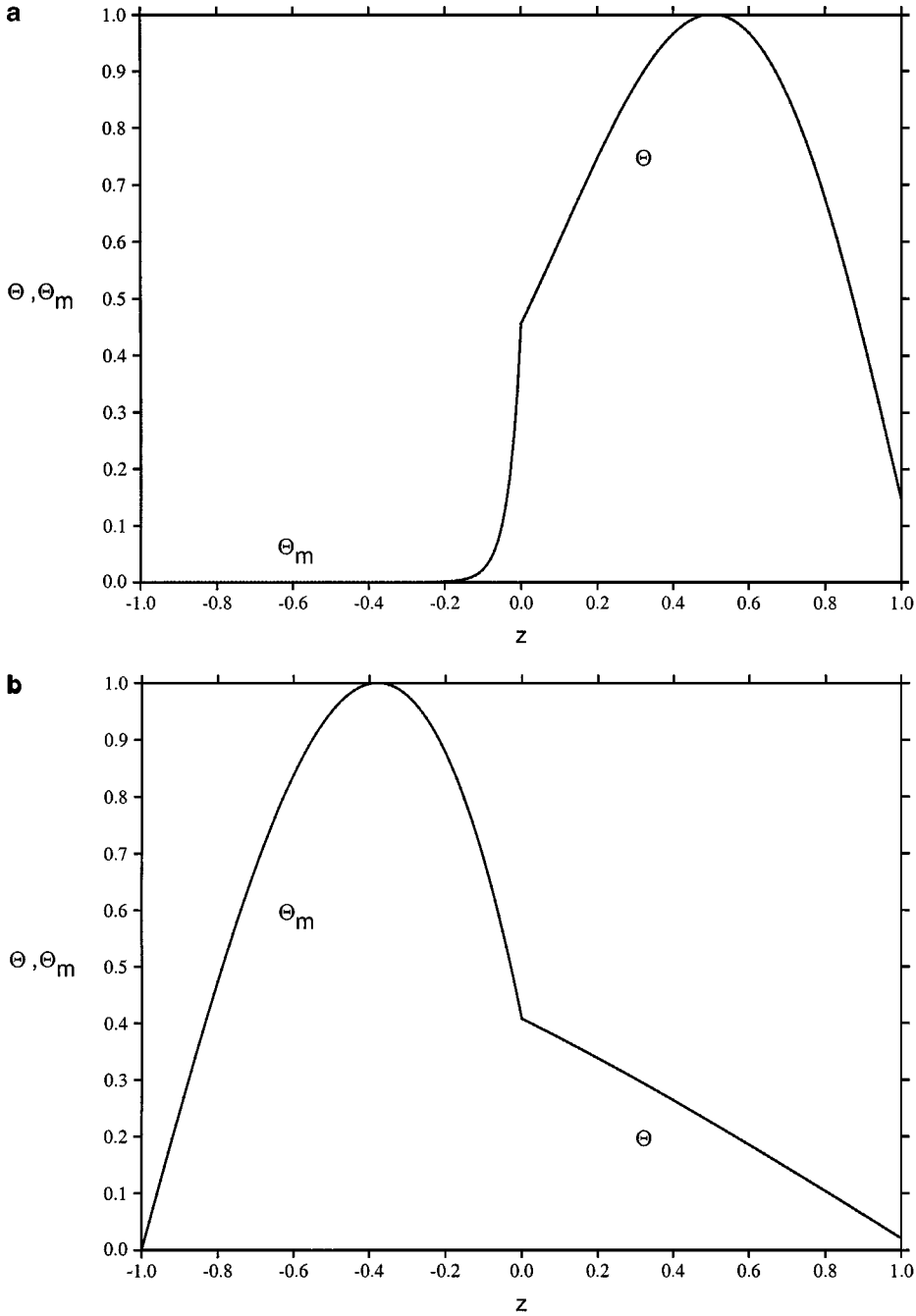

FIG. 7. Dimensional eigenfunctions Θ and Θ_m. (a) $Pr = 6, G_m = 10, \epsilon_T = 0.7, \phi = 0.3, \hat{d} = 0.07, \alpha = 0.1, \delta = 0.002, L = 10, Ma = -400$; (b) $Pr = 6, G_m = 10, \epsilon_T = 0.7, \phi = 0.3, \hat{d} = 0.09, \alpha = 0.1, \delta = 0.002, L = 10, Ma = -300$.

TABLE VI
Maximum Values of Ra_m with the Corresponding Values of a_m, for the Porous Dominated Case

Ma	Ra_m	a_m	$\hat{d}$
0	−30.63	2.7	.01
−100	−29.88	2.7	.01
−200	−29.10	2.7	.01
−300	−28.28	2.7	.01
−400	−27.43	2.7	.01
0	−35.35	3.0	.005
−100	−34.08	3.0	.005
−200	−32.66	3.0	.005
−300	−31.08	3.0	.005
−400	−29.30	3.0	.005
0	−36.49	3.0	.004
−100	−35.12	3.0	.004
−200	−33.56	3.0	.004
−300	−31.79	3.1	.004
−400	−29.72	3.1	.004

Note. $Pr = 6, G_m = 10, \epsilon_T = 0.7, \phi = 0.3, \alpha = 0.1, \delta = 0.002, L = 10$.

5. CONCLUSIONS

In this paper we have implemented a D^2 variant of the Chebyshev tau numerical method and have derived accurate results for the onset of convection in a two-layer system comprising a porous layer over which lies a layer of fluid. The Chebyshev tau method is very important for this general class of problem since it is highly accurate, the eigenfunctions are easy to generate, and it is easily generalised to the multilayer situation where there are many porous–fluid layers superposed. The Chebyshev method used here also yields as many eigenvalues in the spectrum as one desires. This is particularly important in that for convection problems of current interest, it is often the case that the eigenvalues change positions, one eigenvalue which is dominant in a certain region of parameter space being replaced by another in another parameter region. Such effects have already been witnessed in a single layer of fluid or in a single layer of saturated porous material (see Straughan and Walker [20], and Tracey [21] respectively). The extension to the multiporous–fluid layer case has potential for industrial application in making composite materials (see, e.g., the models in Blest *et al.* [2, 3]).

We have investigated in detail the effect of surface tension on the onset of instability. We have also extended the boundary conditions of Chen and Chen [4] to allow for the possibility of oscillatory instabilities. However, we have vindicated their choice of setting $\sigma = 0$ since we have shown numerically that instability does occur via stationary convection, at least for the heated-below situation considered here. In particular, we show that surface tension is increasingly important when the depth of the fluid layer is relatively large or also when the depth of the fluid layer is relatively very thin. In the latter situation our results provide quantitative evidence that Nield's [14] model does represent a realistic situation for convection in a porous medium with a free surface overlain by a thin film of fluid.

ACKNOWLEDGMENT

This work was supported by Leverhulme Research Grant RF & G/9/2000/226.

REFERENCES

1. G. S. Beavers and D. D. Joseph, Boundary conditions at a naturally permeable wall, *J. Fluid Mech.* **30**, 197 (1967).
2. D. C. Blest, B. R. Duffy, S. McKee, and A. K. Zulkifle, Curing simulation of thermoset composites, *Composites: Part A* **30**, 1289 (1999).
3. D. C. Blest, S. McKee, A. K. Zulkifle, and P. Marshall, Curing simulation by autoclave resin infusion, *Composites Sci. Technol.* **59**, 2297 (1999).
4. F. Chen and C. F. Chen, Onset of finger convection in a horizontal porous layer underlying a fluid layer, *J. Heat Transfer* **110**, 403 (1988).
5. S. H. Davis, Buoyancy-surface tension instability by the method of energy, *J. Fluid Mech.* **39**, 347 (1969).
6. J. J. Dongarra, B. Straughan, and D. W. Walker, Chebyshev tau-QZ algorithm methods for calculating spectra of hydrodynamic stability problems, *Appl. Numer. Math.* **22**, 399 (1996).
7. D. R. Gardner, S. A. Trogdon, and R. W. Douglas, A modified tau spectral method that eliminates spurious eigenvalues, *J. Comput. Phys.* **80**, 137 (1989).
8. G. Lebon and A. Cloot, Effects of non-uniform temperature gradients in Bénard–Marangoni's instability, *J. Non-Equilib. Thermodyn.* **6**, 15 (1981).
9. G. B. McFadden, B. T. Murray, and R. F. Boisvert, Elimination of spurious eigenvalues in the Chebyshev tau spectral method, *J. Comput. Phys.* **91**, 228 (1990).
10. G. McKay, Onset of buoyancy-driven convection in superposed reacting fluid and porous layers, *J. Eng. Math.* **33**, 31 (1998).
11. D. A. Nield, Onset of convection in a fluid layer overlying a layer of a porous medium, *J. Fluid Mech.* **81**, 513 (1977).
12. D. A. Nield, The boundary correction for the Rayleigh–Darcy problem: Limitations of the Brinkman equation, *J. Fluid Mech.* **128**, 37 (1983).
13. D. A. Nield, The limitations of the Brinkman–Forchheimer equation in modelling flow in a saturated porous medium and at an interface, *Int. J. Heat Fluid Flow* **12**, 269 (1991).
14. D. A. Nield, Modelling the effect of surface tension on the onset of natural convection in a saturated porous medium, *Transp. Porous Media* **31**, 365 (1998).
15. D. A. Nield, Instability and turbulence in convective flows in porous media, in *Nonlinear Instability, Chaos and Turbulence*, edited by L. Debnath and D. N. Riahi (WIT Press, Boston, Southampton, 1998), pp. 225–276.
16. D. A. Nield and A. Bejan, *Convection in Porous Media* (Springer-Verlag, New York 1999).
17. L. E. Payne and B. Straughan, Analysis of the boundary condition at the interface between a viscous fluid and a porous medium and related modeling questions, *J. Math. Pures Appl.* **77**, 317 (1998).
18. Y. Qin and P. N. Kaloni, Creeping flow past a porous spherical shell, *Z. Angew. Math. Mech.* **73**, 77 (1993).
19. B. Straughan and D. W. Walker, Two very accurate and efficient methods for computing eigenvalues and eigenfunctions in porous convection problems, *J. Comput. Phys.* **127**, 128 (1996).
20. B. Straughan and D. W. Walker, Multi component diffusion and penetrative convection, *Fluid Dyn. Res.* **19**, 77 (1997).
21. J. Tracey, *Stability Analyses of Multicomponent Convection–Diffusion Problems*, Ph.D. thesis (Glasgow Univ., 1997).
22. A. Zebib, Removal of spurious modes encountered in solving stability problems by spectral methods, *J. Comput. Phys.* **70**, 521 (1987).